Cellulose (2023) 30:1543–1552
https://doi.org/10.1007/s10570-022-04970-3

ORIGINAL RESEARCH

Roll stamped Ni/MWCNT composites for highly reliable cellulose paper-based strain sensor

Xue Qi · Paolo Matteini · Byungil Hwang · Sooman Lim

Received: 22 June 2022 / Accepted: 23 November 2022 / Published online: 1 December 2022

Abstract Printing technology for electronic devices has garnered considerable attention owing to its rapid and massive productivity under ambient conditions. In this study, a facile approach is proposed for manufacturing cellulose paper-based strain sensors with Ni/multi-walled carbon nanotube (MWCNT) composites using roll stamping technology. This process enables the fabrication of stable sensing structures owing to the formation of stable Ni core-enveloping structures in the MWCNT interlacing network. In particular, the rheological properties of the composites revealed shear thinning and thixotropic behavior, which resulted in fine printing of the sensing electrodes. Furthermore, the shape of the printed patterns, imparted by the pattern morphology, significantly influenced the strain-sensing performance. In particular, the Ni/MWCNT composite-based strain sensor exhibited a higher gauge factor of 13.9, with a high sensing recovery of 90.4% and stability over 23,500 bending cycles.

Keywords Ni/MWCNT composites · Strain sensor · Roll stamping · 3D printing · Paper-based sensor · Sensing stability

Supplementary Information The online version contains supplementary material available at https://doi.org/10.1007/s10570-022-04970-3.

X. Qi · S. Lim (✉)
Department of Flexible and Printable Electronics, LANL-JBNU Engineering Institute, Jeonbuk National University, Jeonju 54896, Republic of Korea
e-mail: smlim@jbnu.ac.kr

X. Qi
Shenzhen Key Laboratory of Flexible Printed Electronics Technology, School of Materials Science and Engineering, Harbin Institute of Technology (Shenzhen), Shenzhen 518055, China

P. Matteini
Institute of Applied Physics "Nello Carrara", National Research Council, Via Madonna del Piano 10, 50019 Sesto Fiorentino, Italy

B. Hwang (✉)
School of Integrative Engineering, Chung-Ang University, Seoul 06974, Republic of Korea
e-mail: bihwang@cau.ac.kr

Introduction

An environment friendly cellulose paper-based strain sensor that converts mechanical strain into an electrical output signal has been widely utilized in various applications for tracking human movement, monitoring mechanical deformation, and in water-containing circumstances (Liu et al. 2017a, b; Qi et al. 2020b). To improve the performance of the cellulose-paper-based strain sensor, functional conductive materials were used to realize a change in resistance according to mechanical deformation. Au or Ag nanowires (Gong et al. 2015; Hwang et al. 2022; Jiang et al. 2019; Najafabadi et al. 2014), graphene (Mehmood

et al. 2020; Zhao et al. 2013) and ZnO nanowires (Desai and Haque 2007; Jenkins and Yang 2017) have been previously used. However, the performance of flexible paper-based strain sensors using these materials with conventional processing methods is limited because of their low electrical conductivity, scalability, and applications (Qi et al. 2020a; Qi and Lim 2022). Recently, carbon nanotube (CNT) composites have circumvented these limitations and exhibited excellent mechanical and electrical properties for use in strain sensors (Sezer and Eren 2019; Song et al. 2020; Spitalsky et al. 2010). However, because problems of aggregation emerge on the part of CNTs (Mayappan et al. 2016; Yang et al. 2017), functionalized metal–CNT composites have been suggested for suitable dispersal and bonding structures (Li et al. 2019). Among the various choices, Ni is suitable for deposition on CNT surfaces in diverse forming processes to improve its functionality (Freitas et al. 2012; Mandal and Mondal 2018; Yim et al. 2016). However, Ni/multi-walled CNT (Ni/MWCNT) composites formulated by solution processes have rarely been employed in cellulose paper-based strain sensors to improve their performance.

Various types of printing or coating technologies can be used for the fabrication of cellulose paper-based flexible strain sensors, including screen printing, inkjet printing, and roll-based imprinting processes (Qi et al. 2020b; Wei et al. 2015). Among these, imprinting processes are attractive for the fabrication of such sensors owing to their high productivity. However, conventional imprinting processes using flat-type stamps suffer from low efficiency, nonuniformity, and small replication areas (Lan et al. 2010). In contrast, roll-based imprinting is advantageous because it works continuously, leading to higher uniformity, lower loading pressure, simpler structure, higher efficiency, and lower fabrication cost (Lan et al. 2008).

In this study, Ni/MWCNT composite is synthesized through a sequential formulation process to function as ink for the roll stamping process in the fabrication of cellulose paper-based strain sensors. The rheological properties of the composite are systematically studied to confirm the printability. Roll stamping patterns are fabricated using a digital light processing (DLP)-based 3D printer to realize high pattern quality with low cost. Subsequently, the Ni/MWCNT composites are printed on paper, and the performance of the printed strain sensor is evaluated. The cellulose paper-based Ni/MWCNT flexible strain sensor exhibits a gauge factor of 13 and excellent bending stability for 23,500 cycles.

Experimental section

Raw materials

Ni (CAS-No.:7440-02-0, MW:58.69 g mol^{-1}, < 50 µm, 99.7% trace metals), Butylcarbitol and polyvinyl butyral (PVB) terpolymers (CAS-No.:63148-65-2, 432.90 g mol^{-1}, 99.99% purity) were purchased from Sigma-Aldrich. MWCNTs (US Research Nanomaterials, Inc.) utilized have an external diameter of 5–15 nm and purity higher than 95%. Fluorosurfactant (FC-4430) was purchased from 3M (USA). SteroColl ® HS, FoamStar® SI 2213, and Hydropalat® WE 3475 were obtained from BASF. The cellulose paper was in A4 format and was purchased from Double-A PLC. In Figure S1, A4 paper shows a large C–O–C peak, which results from cellulose or holocellulose. The second largest peak corresponds to the C=O vibration, which can be due to lignin. Thus, A4 paper was considered to have a high lignin content. Indeed, the mass ratio of lignin to holocellulose was 1:1, as analyzed using the Van Soest procedure (Yun et al. 2018).

Preparation of Ni/MWCNT and Ni composites

A simple, inexpensive, room-temperature process was used to prepare the Ni/MWCNT composite. The Ni to MWCNT ratio was 20:1. The weight ratios of the Ni/MWCNT composites, dispersant (FC-4430, providing low surface tension), solvent-resin vehicle (butyl carbitol and PVB), thickener (Sterocoll HS, rheology modifier), defoaming agent (FoamStar SI 2213), and wetting agent (Hydropalat WE 3475) were 50.8:0.1:47:1:0.1:1. These materials were mixed using a vortex agitator (Daihan Scientific) at 1000 revolutions *per* minute for 12 h. The composites were added to a planetary centrifugal bubble-free mixer (ARE-310, THINKY U.S.A., Inc.) for 20 min and then degassed three times for 5 min. A control group of nickel composites was also prepared using the same process. The weight ratios of Ni powder, dispersant (FC-4430, providing low surface tension),

solvent-resin vehicle (butyl carbitol and PVB), thickener (Sterocoll HS, rheology modifier), defoaming agent (FoamStar SI 2213), and wetting agent (Hydropalat WE 3475) were 50.8:0.1:47:1:0.1:1.

Roll stamping of paper-based strain sensor with Ni/MWCNT composites

A flexible strain sensor with micron-scale electrodes was fabricated to confirm the applicability of the roll stamping method to strain sensors. The film thickness of 0.05 mm was evenly coated on the steel plate using a doctor blade. The roller rolls at a speed of 15 mm s^{-1} to dip the composite and then transfers the composite to the paper substrate to complete the stamp action. The nip pressure was controlled by adjusting the gap between the roll and substrate.

Characterization

The water contact angle was analyzed using the sessile drop method with surface electro-optics (Phoenix 300 Touch, Korea). The viscosity of the Ni/MWCNT composite was measured using a hybrid rheometer (Discovery HR-3, USA) with a 25 mm parallel plate geometry (Peltier plate Steel—107199) and a 100 μm gap. All measurements were performed at room temperature (25 °C). The structure of the Ni/MWCNT on paper was determined using X-ray diffraction (XRD, X'pert Pro Powder, Netherlands) analysis with Cu Kα radiation (λ = 1.5405 Å) at 2θ between 5° and 80° with a scan step size of 0.033°. A source meter (Keithley 2400, USA) with a current signal system voltage of 0.1 V was used to test the durability of the sensor using a bending system (OWIS PS 10-32 Germany) at a speed of 10 mm s^{-1}. The bending radius was 20.28 mm after 23,500 cycles. The morphology of the composite films was analyzed by field-emission scanning electron microscopy (FE-SEM, SUPRA 40VP, Carl Zeiss) at the Center for University-Wide Research Facilities (CURF) at Jeonbuk National University. Roll stamping patterns were fabricated using a DLP-based 3D printer (Carima IMC, Republic of Korea) by curing photopolymer urethane resin (CFY063W, Carima) at the rate of 0.05 mm *per* layer with an exposure time of 1 s per layer.

Results and discussion

Figure 1a–c show a schematic cross-section of the roll stamping reel, an image of the cellulose paper-based Ni/MWCNT sensors, and the schemes of various 3D printed templates used for roll stamping, respectively. The substrates obtained by DLP-type 3D printing have various advantages such as low cost, diversified design elements, simplified production process, and printing accuracy.

Figure 2a shows an image of the Ni/MWCNT composite and a schematic representation of the

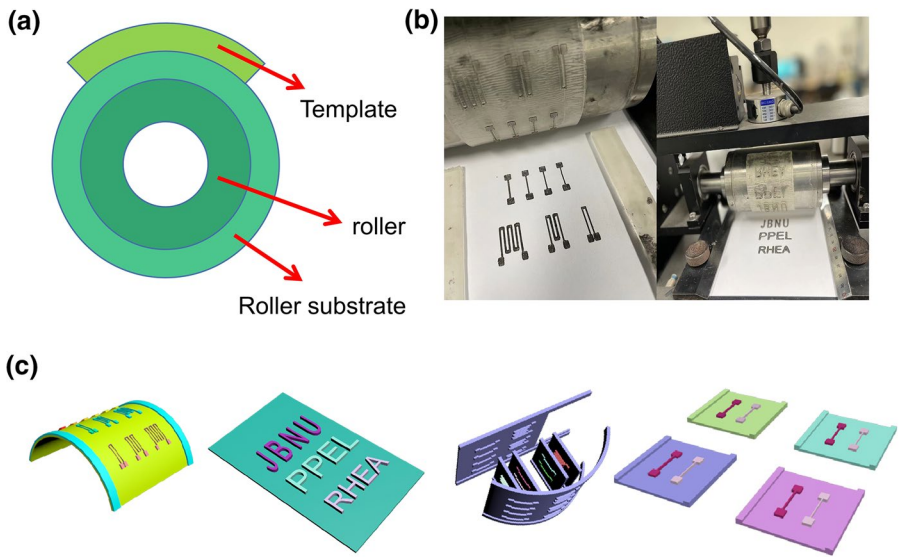

Fig. 1 **a** Schematic cross-section of a roll stamping reel, and **b** real image of the roll stamping process for cellulose paper-based Ni/MWCNT sensors. **c** Various 3D printing templates for roll stamping

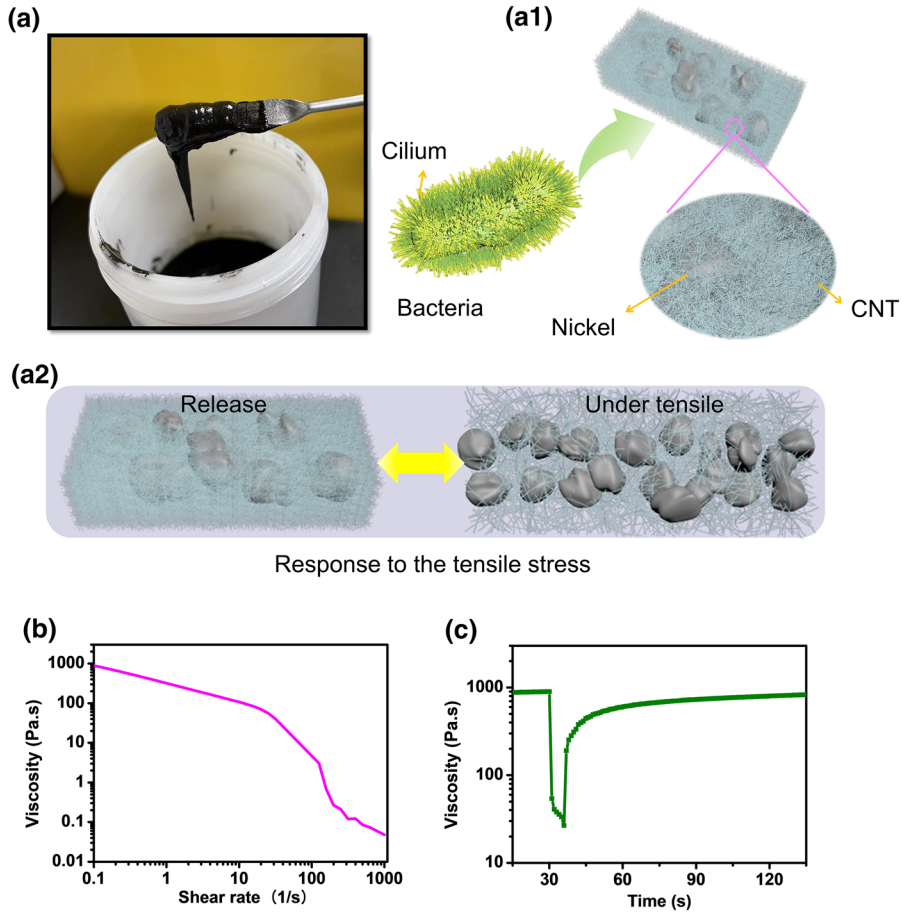

Fig. 2 **a** Photograph of Ni/MWCNT composite, **a-1** schematic diagram of bioengineering design composite and **a-2** response to the tensile stress **b** Shear thinning behavior of Ni/MWCNT composite. **c** Thixotropic behavior of Ni/MWCNT composite

bionic design. The formation of a dense network of MWCNTs effectively overcomes the gaps between the nickel particles, particularly in the case of external tension, which guarantees an effective electronic path. MWCNTs played a similar role to the cilia of bacteria (Fig. 2a-1). There are two major classes of cilia: motile and non-motile cilia (Falk et al. 2015). In addition to motor functions, cilia also play a role in cellular communication and molecular transport. Immobile cilia are sensory organs that detect signals and mediate their transfer in sensory neurons (Capelson and Hetzer 2009; Girirajan et al. 2011). MWCNTs, similar to bacterial cilia, increase electron paths and contact area, promoting the stability of the sensor, especially under tensile stress (Fig. 2a-2). To investigate the printability of the Ni/MWCNT composite, as shown in Fig. 2b, various rheological properties were evaluated; the tests were repeated three times and representative results were obtained. In Fig. 2b, the steady-state test reveals shear-thinning behavior with increasing shear rate, which is generally observed in printing processes where an applied shear force exists (Reinhardt et al. 2018). Figure 2c illustrates the thixotropic behavior of the composite simulating the roll stamping process by performing peak-hold experiments at different shear rates and three different periods. In the first stage, a shear rate of 0.1 s^{-1} was continuous for 30 s to simulate loading the composite on the roller, followed by an appropriate shear rate of 100 s^{-1}, which indicated that the composite transfer action performed. Further, the shear rate was decreased from 100 to 0.1 s^{-1} and run for 100 s to simulate the deposition of the composites on the substrate. The elasticity of the composite was evaluated according to the recovery rate, which in turn affected the pattern fidelity (Fig. 2c). The results showed that the composite exhibited evident thixotropic behavior over time, and the recovery rate at the leveling point (125 s) was greater than 90%, indicating that the Ni/MWCNT composite had high elasticity. These

phenomena imply that MWCNTs play an important role in reinforcing the inner strength of the composite structure owing to their high aspect ratio and electrostatic attraction to Ni (Kamkar et al. 2020).

To achieve a higher pattern quality in the roll stamping process, a high contact pressure at the nip is required because composite transfer from the stamp to the substrate occurs at the nip. However, Halo effect was observed around printed regions when the nip pressure was adjusted. To investigate this phenomenon, we analyzed the effect of the nip pressure using COMSOL Multiphysics software (version 6.0). In the analysis, the cylinder was subjected to a point load; therefore, the contact pressure distribution and the length of contact between the roll and the substrate based on the applied pressure were considered, as shown in Fig. 3a, which shows the deformed shape and von Mises stress distribution obtained using the penalty contact method for the increase in the nip pressure. As the nip pressure increased, increases in the contact stress, and contact length point were simultaneously increased. The results indicate that although a higher pressure can induce tighter contact, excessive pressure causes uneven solution transfer owing to the deformation of the flexible printing medium at a wider contact point. The details are provided in the supporting materials (S2). After adjusting the pressure, strain sensors with various line widths (200, 300, and 500 µm) at a fixed line length of 12 mm and lengths (27, 50, and 76 mm) at a fixed line width of 300 µm were fabricated. Digital images of roll stamped Ni/MWCNT electrodes with a line width of 500 µm on paper at a magnification of 5x are shown in Fig. 3b. The printed line with fine edges and dense structure demonstrated the high printability of the composite, while considering the rough and

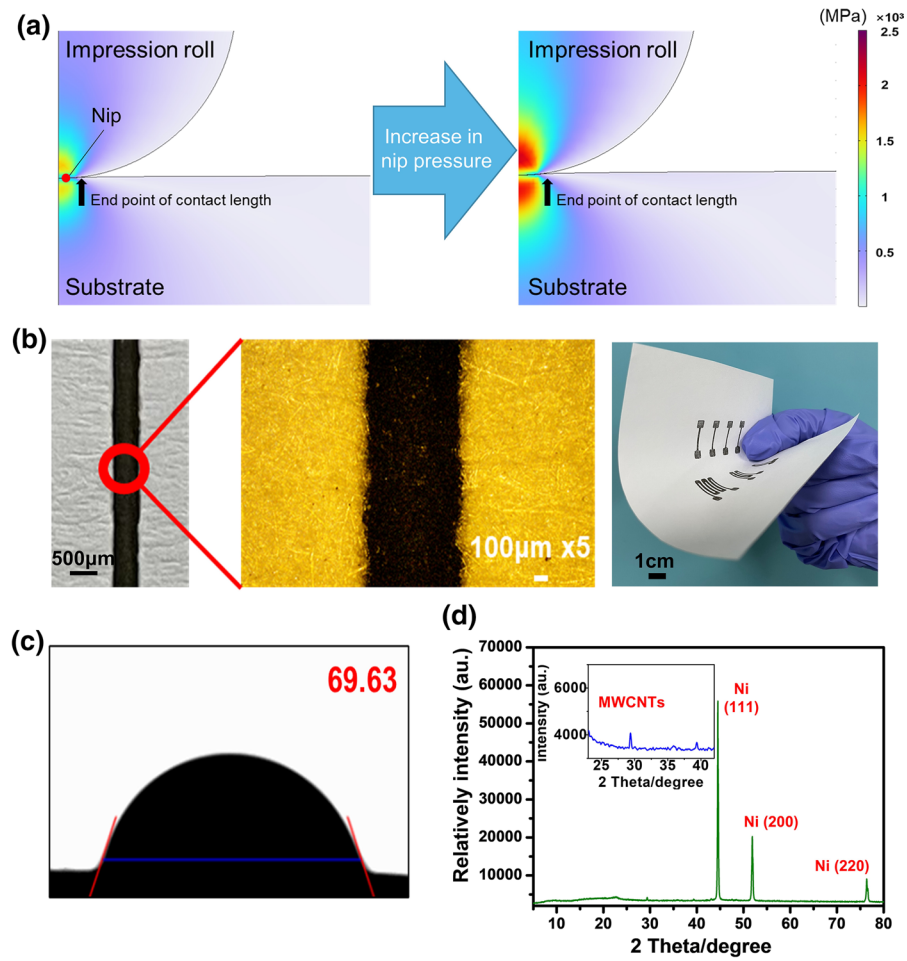

Fig. 3 **a** Deformed shape and von Mises stress distribution obtained using the penalty contact method for the case of applied higher nip pressures. **b** Digital images of sensors with roll stamped Ni/MWCNT electrodes on paper substrate. **c** Static contact angle of DI water on the paper surface. **d** The XRD patterns of the synthesized Ni/MWCNT composite

uneven fiber structure of the paper. Figure 3c shows the contact angle of 69.63° for deionized water on paper, measured using the pendant drop method, substantiating its hydrophilic surface characteristics, where the experiment was repeated more than three times and representative results are shown. In general, the hydrophilicity of paper leads to the diffusion of solvents and affects the resolution of printed electronics (Tortorich et al. 2018). Ni/MWCNT composites with high viscosity, however, can effectively reduce this effect on the print resolution. The XRD patterns of the synthesized nanocomposite are shown in Fig. 3d, in which the experiment was repeated three times. Samples were analyzed in the form of powder in the reflection mode. The main characteristic peaks of Ni (indexed as 111, 200, and 220) and MWCNT (inset), even after drying, indicate that presence of Ni and MWCNT in the composite after drying.

Subsequently, the sensing properties of the printed sensors were investigated (Fig. 4). The electrical performance of the resistive-type sensor following Ohm's law is critical to attain high sensitivity because the sensor consists of electrodes. A linear slope with a change in the morphology of the pattern indicated the uniform conductivity of the strain sensors, as shown in Fig. 4a and b, where the tests were repeated more than three times.

In addition, a sensor with a larger width and shorter length tended to exhibit a higher current, which is reasonable based on Ohm's law. To investigate the sensitivity of the Ni/MWCNT composite printed on cellulose paper, the sensor was subjected to strain in the range of 0.25–0.53%, as shown in Fig. 4c. The experiment was repeated more than three times to confirm the effect. The sensor could detect a minimum strain change of 0.03% in the applied range. The calculated gauge factor (GF), defined as

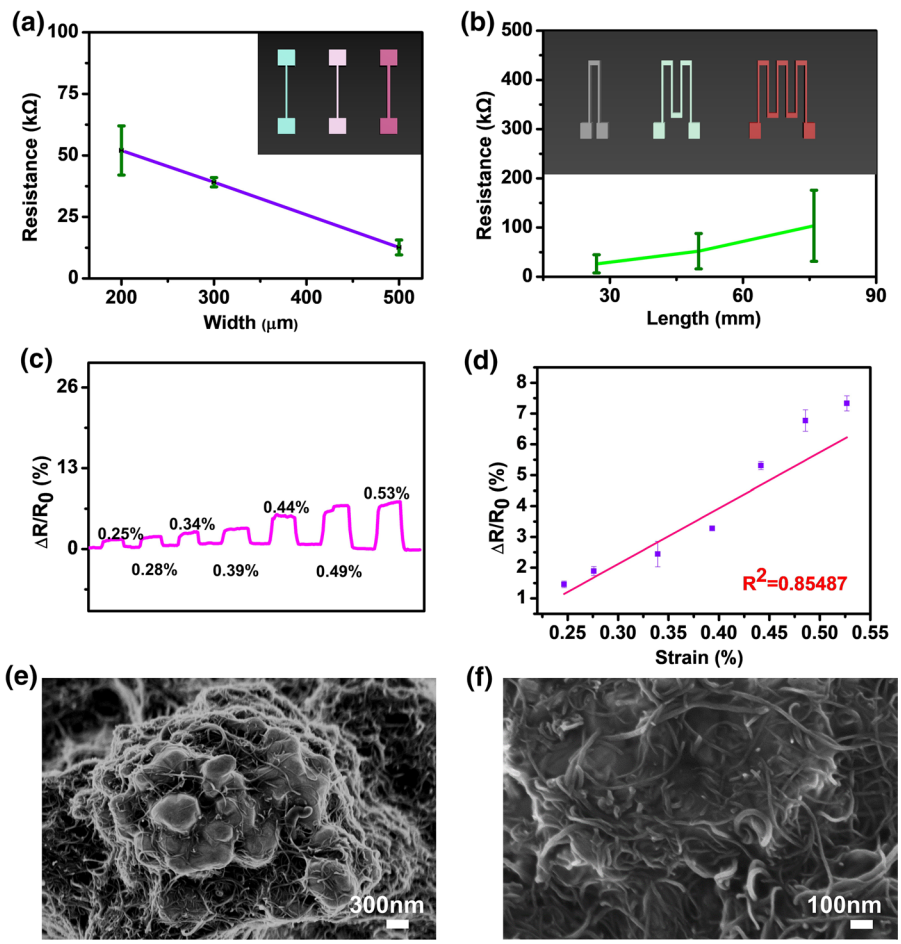

Fig. 4 Measured resistance plots of the roll stamped Ni/MWCNT sensors with line patterns (inset) of various dimensions: **a** variation with the line width **b** variation with the line length. **c** Relative change in the resistance on application of strain with stepwise increase **d** Relative change in the resistance on continuous progressive strain application. FE-SEM images of Ni/MWCNT paper-based sensor: 20,000x (**e**) and 60,000x (**f**)

$(\Delta R/R_0)/\varepsilon$, where R_0 is the resistance of the composite sensor without strain, ΔR is the resistance change under strain, and ε denotes applied strain, was 13.9. This is six times higher than that of commercially available strain sensors, namely, con-copper (55% Cu, 45% Ni; GF: +2.0), nickel–chromium (80% Ni, 20% Cr; GF: +2.0), or Constantan (45% Ni, 55% Cu; GF: +2.0) -based foil-type resistance sensors (Bolton 2021; Litao Liu et al. 2009; Qi et al. 2020a). In addition, the uniform linearity of the sensor was 85%, as shown in Fig. 4d, in which a representative value was obtained after more than three repetitions. The FE-SEM images in Fig. 4e and f show the skein-like morphology of the Ni-MWCNT composite, where Ni clusters serve as core conducting sites to form stable network structures with MWCNT. An average size of Ni cluster was ~3.5 ± 0.6 µm, which was confirmed from the measurement of multiple Ni cluster sizes in the SEM chamber.

Figure 5a shows the relative resistance changes of the Ni/MWCNT sensor at different strain rates under a strain of 0.53%, which exhibits a stable sensing response with a two-fold increase in the strain rate after more than three replicates of the experiment. Figure 5b shows the relative resistance changes of the sensor under strain-release cycle, demonstrating a high sensing recovery of 90.4%. Considering the cyclic stability test under multiple strain applications in one process, the high stability of the sensor was demonstrated by a linearity of 0.85 under continuous and diverse strains within 0.25–0.53% (Fig. 4c). The results were obtained from more than three replicate

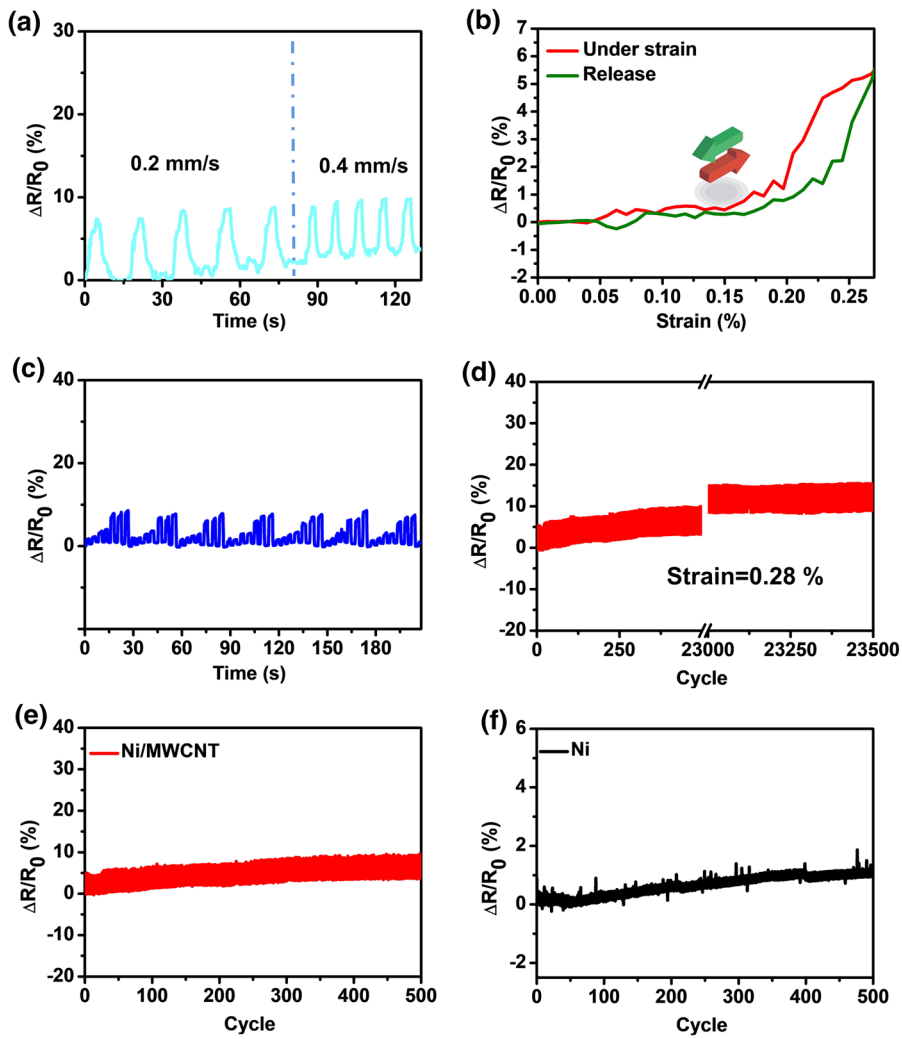

Fig. 5 **a** Relative resistance changes of the Ni/MWCNT sensor at different strain rates under a strain of 0.53%. **b** Relative resistance changes of the sensor under step -release cycle. **c** High stability of the sensor under continuous multiple strain cycles. **d** Durability of the composite under 23,500 cycles with low tensile deformation. Here, $\Delta R/R_0$ is a function of multiple bending and releasing cycles with a strain 0.28% for Ni/MWCNT composite, where ΔR denotes the resistance differences under bending and release and R is the initial resistance in the relaxed state. Durability of composites for 500 cycles with low tensile deformation: **e** Ni/MWCNT composite and **f** Ni

Table 1 Comparison of durability of various paper-based sensors

Type of the sensor	Materials	Bending cycles	References
Paper-based	Graphite	10,000	Liao et al. (2016)
Paper-based	Ag NPs/SiO_2/MWCNT	12,000	Liu et al. (2021)
Paper-based	$Ti_3C_2T_X$ MXene	1000	Bu et al. (2021)
Paper-based	Graphene	1000	Qian et al. (2019)
Paper-based	ITO nanoparticle	1000	Lee & Kim (2019)
Paper-based	Graphene	1000	Qi et al. (2020b)
Paper-based	Carbon black	1000	Liu et al. (2017a, b)
Paper-based	Carbon	2000	Duan et al. (2021)
Paper-based	Carbon	5000	Xia et al. (2019)
Paper-based	Ni/MWCNT	23,500	This work

experiments. Furthermore, to investigate repeatability and durability under multiple strains, repeated stretch-release cycles were applied to the sensors (Fig. 5c), in which uniform stability was observed. The results were obtained from more than three replicate experiments. Figure 5d shows the change in resistance of the sensors, indicating a fully recoverable electrical resistance without hysteresis at a stretching of 0.28% for 23,500 cycles. The results were obtained from more than three replicate experiments. The sensing stability of the Ni/MWCNT paper-based sensor was compared with that of the pure nickel composite, as shown in Fig. 5e and f, where the tests were repeated more than three times and representative results are shown. The Ni/MWCNT sensor showed higher sensitivity and better reversibility after 500 cycles than the pure Ni paper-based sensor. Table 1 shows a comparison of the durability of various reported paper-based sensors; the Ni/MWCNT paper-based sensor showed high bending durability.

Conclusions

A cellulose-paper-based strain sensor with Ni/MWCNT composite was developed using a full-roll stamping process. The formation of stable Ni core-enveloping structures in the MWCNT interlacing network ensured sufficient resistance to the applied strain, and the sensitivity was determined by varying the printed line morphology. The rheological properties of the Ni/MWCNT composite exhibited shear thinning and thixotropic behavior, which are suitable for roll stamping process that require high shear forces. The optimal pattern characteristics of the sensor, including the line width and line length, agreed with the simulated values, which allowed optimization of the printing conditions of the roll stamping process. The paper-based Ni/MWCNT composite strain sensor exhibited a high GF of 13.9 with a high sensing recovery of 90.4%, which is superior to that of commercial sensors. In addition, the printed sensor showed a fully recoverable electrical resistance without hysteresis at a stretching of 0.28% for 23,500 cycles. Consequently, formulated Ni/MWCNT composite has been proposed as a basic platform for producing highly sensitive and stable strain sensors.

Acknowledgments This work was supported by a National Research Foundation of Korea (NRF) grant funded by the Korean government (NRF-2021R1A2C1011248). This research was supported by the Korea Institute for Advancement of Technology (KIAT) grant funded by the Korean Government (MOTIE) (P0002007, 2022 HRD Program for Industrial Innovation).

Authors' contributions XQ: Conceptualization, Methodology, Data curation, Writing—original draft. PM: Investigation, Review and editing. BH: Investigation, Review and editing. SL: Supervision, Investigation, review and editing.

Funding This work was supported by a National Research Foundation of Korea (NRF) grant funded by the Korean government (NRF-2021R1A2C1011248). This research was supported by the Korea Institute for Advancement of Technology (KIAT) grant funded by the Korean Government (MOTIE) (P0002007, 2022 HRD Program for Industrial Innovation).

Availability of data and materials The authors confirm that data supporting the findings of this study are available within the article.

Declarations

Competing interests The authors declare that they have no known competing financial interests or personal relationships that could have influenced the work reported in this study.

Ethics approval and consent to participate None.

Consent for publication We, the undersigned, give consent for the publication of identifiable details, which can include photographs (s) and details within the text to be published in this journal.

References

Bolton W (2021) Chapter 2: instrumentation system elements. In: Bolton WBT (ed) Instrumentation and control systems, 1st edn. Newnes, London, pp 17–70

Bu Y, Shen T, Yang W, Yang S, Zhao Y, Liu H, Zheng Y, Liu C, Shen C (2021) Ultrasensitive strain sensor based on superhydrophobic microcracked conductive $Ti_3C_2T_x$ MXene/paper for human-motion monitoring and E-skin. Sci Bull 66:1849–1857. https://doi.org/10.1016/j.scib.2021.04.041

Capelson M, Hetzer MW (2009) Development and disease. Mol Biol 15:1–9. https://doi.org/10.1038/embor.2009.147

Desai AV, Haque MA (2007) Mechanical properties of ZnO nanowires. Sens Actuators A Phys 134:169–176. https://doi.org/10.1016/j.sna.2006.04.046

Duan Z, Jiang Y, Huang Q, Zhao Q, Yuan Z, Zhang Y, Wang S, Liu B, Tai H (2021) Integrated cross-section interface engineering and surface encapsulating strategy: a high-response, waterproof, and low-cost paper-based bending strain sensor. J Mater Chem C 9:14003–14011. https://doi.org/10.1039/d1tc03031k

Falk N, Lösl M, Schröder N, Gießl A (2015) Specialized cilia in mammalian sensory systems. Cells 4:500–519. https://doi.org/10.3390/cells4030500

Freitas FS, Gonçalves AS, De Morais A, Benedetti JE, Nogueira AF (2012) Graphene-like MoS_2 as a low-cost counter electrode material for dye-sensitized solar cells. J Energy Sustain. https://doi.org/10.1039/c0xx00000x

Girirajan S, Campbell C, Eichler E (2011) 乳鼠心肌提取 HHS public access. Physiol Behav 176:139–148. https://doi.org/10.1111/febs.14068.Intraflagellar

Gong S, Lai DTH, Su B, Si KJ, Ma Z, Yap LW, Guo P, Cheng W (2015) Highly stretchy black gold E-Skin nanopatches as highly sensitive wearable biomedical sensors. Adv Electron Mater 1:1–7. https://doi.org/10.1002/aelm.201400063

Hwang B, Han Y, Matteini P (2022) Bending fatigue behavior of Ag nanowire/Cu thin-film hybrid interconnects for wearable electronics. Facta Univ Ser Mech Eng. https://doi.org/10.22190/FUME220730040H

Jenkins K, Yang R (2017) Mechanical transfer of ZnO nanowires for a flexible and conformal piezotronic strain sensor. Semicond Sci Technol 32:74004–74004

Jiang D, Wang Y, Li B, Sun C, Wu Z, Yan H, Xing L, Qi S, Li Y, Liu H, Xie W, Wang X, Ding T, Guo Z (2019) Flexible sandwich structural strain sensor based on silver nanowires decorated with self-healing substrate. Macromol Mater Eng 304:1–9. https://doi.org/10.1002/mame.201900074

Kamkar M, Nourin Sultana SM, Patangrao Pawar S, Eshraghian A, Erfanian E, Sundararaj U (2020) The key role of processing in tuning nonlinear viscoelastic properties and microwave absorption in CNT-based polymer nanocomposites. Mater Today Commun 24:101010–101010. https://doi.org/10.1016/j.mtcomm.2020.101010

Lan S, Lee H, Ni J, Lee S, Lee M (2008) Survey on roller-type nanoimprint lithography (RNIL) process. Paper presented at the 2008 international conference on smart manufacturing application

Lan S, Song JH, Lee MG, Ni J, Lee NK, Lee HJ (2010) Continuous roll-to-flat thermal imprinting process for large-area micro-pattern replication on polymer substrate. Microelectron Eng 87:2596–2601. https://doi.org/10.1016/j.mee.2010.07.021

Lee DJ, Kim DY (2019) Paper-based, hand-painted strain sensor based on ITO nanoparticle channels for human motion monitoring. IEEE Access 7:77200–77207. https://doi.org/10.1109/ACCESS.2019.2920920

Li Y, Gan G, Huang Y, Yu X, Cheng J, Liu C (2019) Ag-NPs/MWCNT composite-modified silver-epoxy paste with improved thermal conductivity. RSC Adv 9:20663–20669. https://doi.org/10.1039/c9ra03090e

Liao X, Zhang Z, Liao Q, Liang Q, Ou Y, Xu M, Li M, Zhang G, Zhang Y (2016) Flexible and printable paper-based strain sensors for wearable and large-area green electronics. Nanoscale 8:13025–13032. https://doi.org/10.1039/c6nr02172g

Liu L, Ye X, Wu K, Han R, Zhou Z, Cui T (2009) Humidity sensitivity of multi-walled carbon nanotube networks deposited by dielectrophoresis. Sensors 9:1714–1721

Liu H, Jiang H, Du F, Zhang D, Li Z, Zhou H (2017a) Flexible and degradable paper-based strain sensor with low cost. ACS Sustain Chem Eng 5:10538–10543. https://doi.org/10.1021/acssuschemeng.7b02540

Liu H, Qing H, Li Z, Han YL, Lin M, Yang H, Li A, Lu TJ, Li F, Xu F (2017b) Paper: a promising material for human-friendly functional wearable electronics. Mater Sci Eng R 112:1–22. https://doi.org/10.1016/j.mser.2017.01.001

Liu L, Jiao Z, Zhang J, Wang Y, Zhang C, Meng X, Jiang X, Niu S, Han Z, Ren L (2021) Bioinspired, superhydrophobic, and paper-based strain sensors for wearable and underwater applications. ACS Appl Mater Interfaces 13:1967–1978. https://doi.org/10.1021/acsami.0c18818

Mandal P, Mondal SC (2018) Investigation of electro-thermal property for Cu-MWCNT composite coating on anodized 6061 aluminium alloy. Appl Surf Sci 454:138–147. https://doi.org/10.1016/j.apsusc.2018.05.130

Mayappan R, Hassan AA, Ab Ghani NA, Yahya I, Andas J (2016) Improvement in intermetallic thickness and joint strength in carbon nanotube composite Sn–3.5Ag lead-free solder. Mater Today Proc 3:1338–1344. https://doi.org/10.1016/j.matpr.2016.04.012

Mehmood A, Mubarak NM, Khalid M, Walvekar R, Abdullah EC, Siddiqui MTH, Baloch HA, Nizamuddin S, Mazari S (2020) Graphene based nanomaterials for strain sensor application: a review. J Environ Chem Eng 8:103743–103743. https://doi.org/10.1016/j.jece.2020.103743

Najafabadi AH, Tamayol A, Annabi N, Ochoa M, Mostafalu P, Akbari M, Nikkhah M, Rahimi R, Dokmeci MR, Sonkusale S, Ziaie B, Khademhosseini A (2014) Biodegradable nanofibrous polymeric substrates for generating elastic and flexible electronics. Adv Mater 26:5823–5830. https://doi.org/10.1002/adma.201401537

Qi X, Lim S (2022) A screen-printed metal hybrid composite for wireless wind sensing. Nanomaterials 12:972

Qi X, Ha H, Hwang B, Lim S (2020a) Printability of the screen-printed strain sensor with carbon black/silver paste for sensitive wearable electronics. Appl Sci 10:1–10. https://doi.org/10.3390/app10196983

Qi X, Li X, Jo H, Sideeq Bhat K, Kim S, An J, Kang JW, Lim S (2020b) Mulberry paper-based graphene strain sensor for wearable electronics with high mechanical strength. Sens Actuators A Phys 301:111697–111697. https://doi.org/10.1016/j.sna.2019.111697

Qian Q, Wang Y, Zhang M, Chen L, Feng J, Wang Y, Zhou Y (2019) Ultrasensitive paper-based polyaniline/graphene composite strain sensor for sign language expression. Compos Sci Tech 181:107660–107660. https://doi.org/10.1016/j.compscitech.2019.05.017

Reinhardt K, Hofmann N, Eberstein M (2018) The importance of shear thinning, thixotropic and viscoelastic properties of thick film pastes to predict effects on printing performance. In: EMPC 2017: 21st European microelectronics and packaging conference & exhibition 2018-Jan, pp 1–7. https://doi.org/10.23919/EMPC.2017.8346831

Sezer HK, Eren O (2019) FDM 3D printing of MWCNT reinforced ABS nano-composite parts with enhanced mechanical and electrical properties. J Manuf Process 37:339–347. https://doi.org/10.1016/j.jmapro.2018.12.004

Song P, Song J, Zhang Y (2020) Stretchable conductor based on carbon nanotube/carbon black silicone rubber nanocomposites with highly mechanical, electrical properties and strain sensitivity. Compos Part B Eng 191:107979–107979. https://doi.org/10.1016/j.compositesb.2020.107979

Spitalsky Z, Tasis D, Papagelis K, Galiotis C (2010) Carbon nanotube-polymer composites: chemistry, processing, mechanical and electrical properties. Prog Polym Sci 35:357–401. https://doi.org/10.1016/j.progpolymsci.2009.09.003

Tortorich RP, Shamkhalichenar H, Choi J-W (2018) Inkjet-printed and paper-based electrochemical sensors. Appl Sci 8:288

Wei Y, Chen S, Li F, Lin Y, Zhang Y, Liu L (2015) Highly stable and sensitive paper-based bending sensor using silver nanowires/layered double hydroxides hybrids. ACS Appl Mater Interfaces 7:14182–14191. https://doi.org/10.1021/acsami.5b03824

Xia K, Chen X, Shen X, Li S, Yin Z, Zhang M, Liang X, Zhang Y (2019) Carbonized Chinese art paper-based high-performance wearable strain sensor for human activity monitoring. ACS Appl Electron Mater 1:2415–2421. https://doi.org/10.1021/acsaelm.9b00564

Yang L, Liu H, Zhang Y, Yu H (2017) Study on the reliability of carbon nanotube-reinforced Sn–58Bi lead-free solder joints. J Mater Eng Perform 26:6028–6036. https://doi.org/10.1007/s11665-017-3033-8

Yim YJ, Rhee KY, Park SJ (2016) Electromagnetic interference shielding effectiveness of nickel-plated MWCNTs/high-density polyethylene composites. Compos Part B Eng 98:120–125. https://doi.org/10.1016/j.compositesb.2016.04.061

Yun TG, Kim D, Kim SM, Kim ID, Hyun S, Han SM (2018) Mulberry paper-based supercapacitor exhibiting high mechanical and chemical toughness for large-scale energy storage applications. Adv Energy Mater 8:1–9. https://doi.org/10.1002/aenm.201800064

Zhao J, Guang-Yu Z, Shi D-X (2013) Review of graphene-based strain sensors. Chin Phys B 22:57701–57701. https://doi.org/10.1088/1674-1056/22/5/057701